SCIENCE CHINA
Technological Sciences

•Article•

November 2020 Vol.63 No.11: 2292–2304
https://doi.org/10.1007/s11431-019-1523-2

Urban flood inundation and damage assessment based on numerical simulations of design rainstorms with different characteristics

MEI Chao[1], LIU JiaHong[1,2*], WANG Hao[1,2], LI ZeJin[1], YANG ZhiYong[1], SHAO WeiWei[1], DING XiangYi[1], WENG BaiSha[1], YU YingDong[1] & YAN DianYi[1]

[1]*State Key Laboratory of Simulation and Regulation of Water Cycle in River Basin, China Institute of Water Resources and Hydropower Research, Beijing 100038, China;*
[2]*Engineering and Technology Research Center for Water Resources and Hydroecology of the Ministry of Water Resources, Beijing 100044, China*

Received September 15, 2019; accepted January 7, 2020; published online April 24, 2020

In the context of global climate change and urbanization, urban flooding is an important type of natural disaster that affects urban development, especially in China, which is experiencing rapid urbanization. In the past 10 years, urban flooding events have caused huge disaster losses in Chinese cities. This has resulted in significant negative effects on the urban infrastructure, socioeconomic systems, and urban residents, thus causing widespread concern. Studies have confirmed the change in extreme rainstorms is due to the changing environments in many cities globally. Conducting studies on the impact of these rainstorms with different characteristics for urban flooding is valuable for coping with unfavorable situations. In addition, numerical simulations provide an economical and viable means to perform these studies. This paper presents a numerical model of Xiamen Island in China. Simulations were conducted for 12 design rainstorm events with different return periods, rain patterns, and durations. The results indicate that, in the case of an equal rainfall amount, the rainfall intensity is the key factor that affects the inundated area, depth, and damages. However, the rainfall intensity is not the only determining factor; the rainfall pattern also affects the inundations. In regard to the rainfall pattern, a higher rainfall peak coefficient usually leads to severe urban inundation and damage. As a result, the lag time would be shorter, which may further exacerbate the impact of urban flood disasters. The results of this study provide insights into managing flood risks, developing urban flood prevention strategies, and designing flood prevention measures.

urban flood, flood damage assessment, flood disaster management, numerical simulations, design rainstorms

Citation: Mei C, Liu J H, Wang H, et al. Urban flood inundation and damage assessment based on numerical simulations of design rainstorms with different characteristics. Sci China Tech Sci, 2020, 63: 2292–2304, https://doi.org/10.1007/s11431-019-1523-2

1 Introduction

Urban flooding is a global issue that is gaining widespread attention in the context of climate change and urbanization [1,2]. As a country with a high speed of development, China has experienced rapid urbanization in recent years and has faced many severe urban flooding disasters [3–5]. Notable examples of recent urban flooding in China include events in Beijing in July 2012, Wuhan in July 2016, and Shenzhen in April 2019. All of these events caused tremendous property losses and casualties, thus resulting in widespread concern [6–8]. Urban flooding disasters also occur frequently in many southeastern Asian countries [9,10], which have geographical and socioeconomic conditions similar to China.

*Corresponding author (email: liujh@iwhr.com)

Frequent urban flooding events and a large number of disasters indicate that urban flooding is one of the most important factors that hinders urban development [11,12]. More in-depth research is needed to assist city managers in making better decisions about how to prepare for and cope with future flooding events.

In recent years, many studies have shown that global climate change and urbanization has caused significant changes in rainfall in urban areas [13,14]. The findings from these studies suggest that the frequency of extreme rainstorms in urban areas has increased significantly [15] and has led to more frequent urban flooding events and a higher amount of associated damage in many cities [16,17]. Extreme rainfall events are known to be a key hazard for urban flooding; greater rainfall leads to more serious flood disasters. However, little information is available on how increasing rainfall affects urban flooding and how other rainfall characteristics (e.g., intensity, pattern, and duration) influence urban flooding. In fact, environmental change not only causes heavier and more frequent extreme urban rainfall, but it also affects many essential characteristics of extreme urban rainfall [18]; the latter's effects seem to be more important. The rapid expansion of urbanization and urban agglomeration is likely to lead the underlying surface change and increasing of flood risk [19]. Estimating the disaster damage is complex for urban floods, which requires detailed investigations about urban socioeconomic factors [20]. The HAZUS-MH model is a powerful hazard loss estimation model, which includes a library of more than 900 damage curves for a variety of buildings and infrastructure. This model has been widely used in many fields [21]. Jamali et al. [22] developed a flood inundation model called RUFIDAM, which adopts a stage-depth damage curve method to assess the financial damage. These studies provide various damage assessment models and most of the principles translate water depths into damage values through empirical equations [23,24]. This study analyzed the damage losses from the viewpoint of direct economic losses; therefore, analyzing the impact of different rainfall characteristics on urban flooding and assessing the damage losses would help city managers to better cope with urban flooding under changing environments [25].

As an advanced urban flood management tool, numerical simulation plays an important role in urban flood infrastructure planning and design, flood forecasting, early warning, and urban flood risk assessment [26,27]. A robust urban flood model can simulate a variety of scenarios and an unlimited number of urban floods. The effects of different rainfall characteristics on urban flooding can be analyzed by comparing the results of flood simulations under different scenarios. Finally, it can provide technological support for urban flood management in the context of climate change [28,29].

Many urban stormwater models have been applied to urban flood simulation, such as SWMM [30], TELEMAC-2D [31], LISFLOOD-FP [32], and MIKE Flood [33]. Selection of an appropriate model depends on the user's preferences, data accessibility, and the nature of the research questions [34]. TELEMAC-2D was selected for urban inundation modelling in this study. TELEMAC-2D is a two-dimensional flood model developed by the French National Hydraulics and Environment Laboratory [35]. It solves the complete shallow water equations [36] and has a rainfall-runoff simulation function with high stability and applicability to flood modelling, which has been widely used in urban flooding and coastal storm surge simulations [31,37].

The objectives of this study were to set up a flood inundation model of the study area based on TELEMAC-2D and to simulate 12 different design rainstorms with different rainfall return periods, patterns, and durations. The urban inundation model was applied to the 12 design rainstorms, and the effects of the rainfall characteristics on the urban inundation were identified by comparing the statistical results for urban inundation and the disaster damage. It should be pointed out that serious urban flood disasters caused by short-duration rainstorms are difficult to prevent. This study focused on the urban flood inundation and damage assessment based on rainstorms with different characteristics. In addition, the duration of the design storm scenarios was less than 6 h.

2 Material and methods

2.1 Study area and data

Xiamen Island (Figure 1) is a part of Xiamen city in Fujian Province, located in the southeastern coastal area of China and has an area of 142.9 km^2. The terrain of Xiamen Island is high in elevation in the south and low in the north. Xiamen Island has a subtropical climate with an average annual rainfall of 1513.3 mm (based on data from 1965–2015). However, the spatial and temporal variations in precipitation are large, and the rainfall distribution throughout the year is uneven. Most of the annual rainfall is concentrated in the period from May to August, which accounts for approximately 70% of the total annual rainfall. The urbanization rate of Xiamen Island is greater than 80% and the underlying surface impermeability rate is as high as 78%. There are few rivers on the island, and most of them are channelized and concealed. Xiamen Island suffers from severe urban flooding during every rainy season, especially during typhoons. It has been reported that there have been more than 10 serious urban flood events on the island in the past five years.

The data used in this study includes data on land use, soil type, and elevation, all of which are important for constructing urban flood models. The remote sensing (RS)

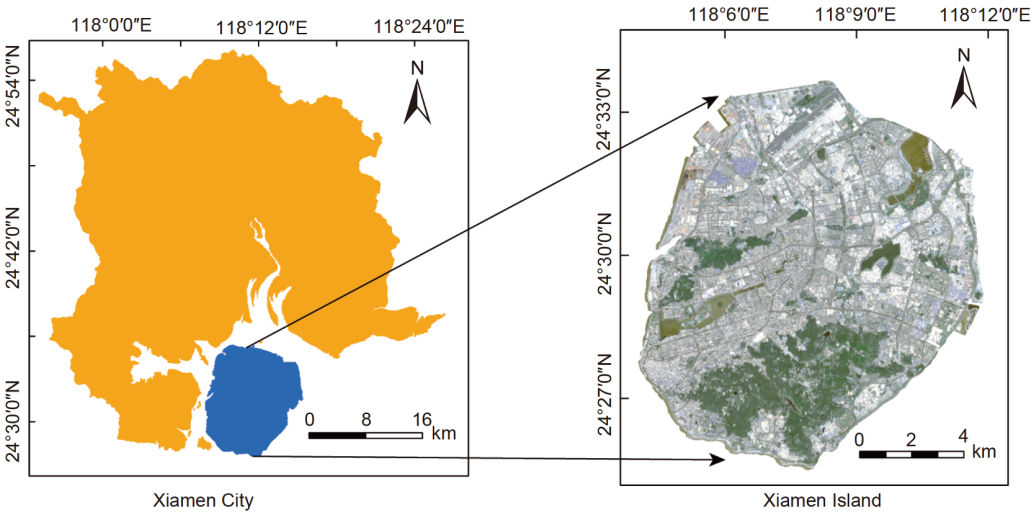

Figure 1 (Color online) Location of the study area.

technology in urban flood simulations has been widely applied [38]. Land use data was obtained through satellite remote sensing image data interpretation. GF-1 satellite remote sensing data with a resolution of 16 m was downloaded from the China Satellite Resource Application Center (http://www.cresda.com/CN/). The RS image was used to produce land use type data based on ENVI 5.3 software by the Support Vector Machine Classification. This is one of the supervision classification methods for land use classification. There are enough regions of interests (ROI) for the visual interpretation method. When it is selected, it can guarantee the accuracy of the land use classification. The results were further evaluated based on comparisons with images from Google Earth. The results show that the land use classification is rational and meets the study's requirements. The land use types on Xiamen Island were classed into five types: woodland, road, water, building, and other (Figure 2(a)). The soil type data was downloaded from the Cold and Arid Science Data Center website (http://westdc.westgis.ac.cn/data/) and was reclassified based on the soil classification criteria of the Soil Conservation Service Curve Number (SCS-CN) model (Figure 2(b)). The elevation data with a resolution of 30 mm (Figure 2(c)) was downloaded from the Geospatial Data Cloud website (http://www.gscloud.cn/). The basic data used in this study was processed using the ENVI 5.3 and ArcGIS 10.4 software platforms. These three datasets have different characteristics and different resolutions. In this paper, when considering the tradeoff between the computational efficacy and the model performance, the three datasets were resampled so the resolution was 30 m. When constructing the models, important parameters, such as the manning coefficient and the CN value, were determined based on the land use and soil type.

Figure 3 illustrates the framework for the flood inundation assessment for 12 rainfall storm designs in this study.

In this study, the design rainstorm formula for Xiamen Island, shown in eq. (1), was used to generate rainfall data with different characteristics. The design rainstorm events

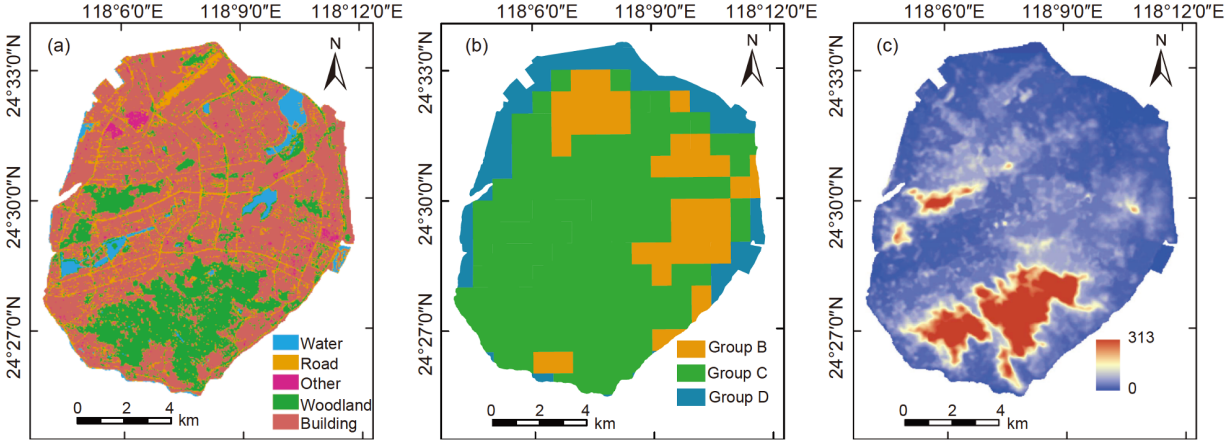

Figure 2 (Color online) Basic data used in this study. (a) Land use types; (b) hydrological soil groups; (c) DEM data (m).

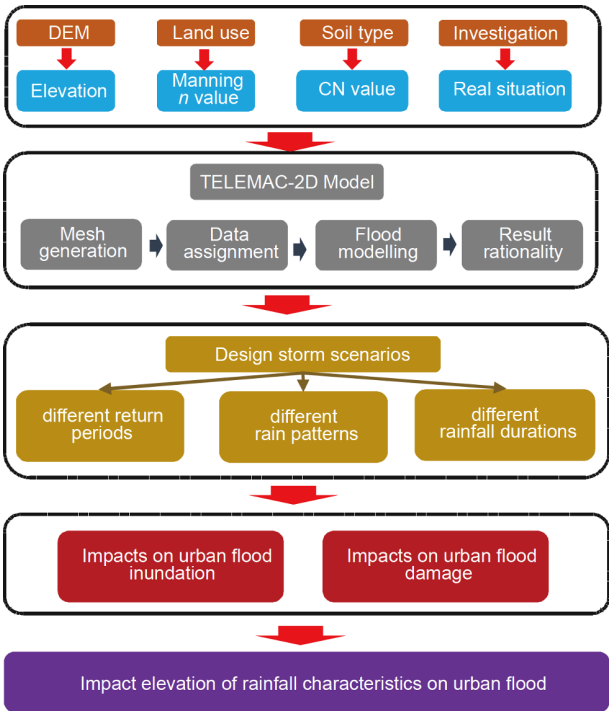

Figure 3 (Color online) Framework of the urban flood assessment under design storms with different characteristics.

generated were used as input data for the urban flood model. Urban flood simulations under different scenarios were then carried out. The design rainstorm formula for Xiamen Island is as follows [39]:

$$q = \frac{928.5 \times (1 + 0.716 \lg P)}{(t + 4.4)^{0.535}}, \quad (1)$$

where q is the rainstorm intensity, L/(s hm^2); P is the return period, a; and t is the rainfall duration, min.

One study reported that rainstorms in Xiamen mostly occur during the rainy season and most of these storms are from typhoons, which is usually a single-peak rainfall [40]. Based on our understanding of the rainstorm laws in Xiamen, after comparing the different design rain patterns, the Chicago rain formula [41] was employed in this study to design the rainstorm process. The Chicago rain formula has been widely used in urban flood management and urban drainage infrastructure designing [42,43]. The Chicago design rainstorm formula was from a technical report according to the Department of Climate of Xiamen City in 2016. This formula has been successfully applied and is reliable [39].

Based on a previous study and established model by Liu et al. [39], further research needs to be conducted to achieve a more in-depth analysis of the impact of rainfall characteristics on urban flooding. For this purpose, three typical characteristics of a design rainstorm for this study were focused on the return period, rain pattern, and rainfall duration [25]. The design rainstorms were classified in three ways: by different return periods (S1), different rain patterns (S2), and different rainfall durations (S3). There were 12 design rainfall events in total. The 12 rainfall events are summarized in Table 1 and more details are provided in Figure 4. It should be noted that a 100-yr design rainstorm with a rain peak coefficient of 0.4 and a duration of 2 h appears in all three scenarios. However, for clarity of presentation, this event is referred to by different labels for the different scenarios, namely S1R4, S2R2, and S3R2.

The framework for this study is presented in Figure 3. The urban flood inundation and damage for the design rainstorms with different characteristics was elevated based on the numerical simulations and scenario analysis.

2.2 TELEMAC-2D model

TELEMAC-MASCARET was developed by the French National Hydraulics and Environment Laboratory, and TELEMAC-2D model is a two-dimensional (2D) module in the TELEMAC-MASCARET series (http://www.opentelemac.org/) [44]. The model solves the 2D depth-averaged Saint-Venant equations for free surface flow, continuity, and momentum along the x and y axes [45]. This model is widely used for hydrodynamic and coastal storm surge simulations [31,37]. The main results at each node for the computational mesh are the depth of the water and the depth-averaged velocity components. TELEMAC-2D solves the Saint-Venant equations based on the finite element method (FEM). Several well-balanced classical discretization schemes were adapted, which provide a proper choice for different numerical scenarios. Furthermore, the code source is open and free; therefore, it is helpful for researchers to develop the model on urban flood situations with their actual requirements. TELEMAC-2D was maintained and updated by a technological team. The seventh version of the model with the FEM scheme was adapted in this research. The governing equations for TELEMAC-2D are as follows:

$$\frac{\partial h}{\partial t} + \frac{\partial (hu)}{\partial x} + \frac{\partial (hv)}{\partial y} = 0, \quad (2)$$

$$\frac{\partial u}{\partial t} + u\frac{\partial u}{\partial x} + v\frac{\partial u}{\partial y} = -g\frac{\partial Z}{\partial x} + F_x + \frac{1}{h}\mathrm{div}(hv_e \nabla u), \quad (3a)$$

$$\frac{\partial v}{\partial t} + u\frac{\partial v}{\partial x} + v\frac{\partial v}{\partial y} = -g\frac{\partial Z}{\partial y} + F_y + \frac{1}{h}\mathrm{div}(hv_e \nabla y), \quad (3b)$$

where h is the water depth; u and v are the velocity com-

Table 1 Design storm scenarios with various return periods, peak coefficients, and rainfall durations. Notes: r refers to the rain peak coefficient, P refers to the return period, and t refers to the rainfall duration

Scenarios	R1	R2	R3	R4
S1 (r=0.4, t=2 h)	P=10	P=20	P=50	P=100
S2 (P=100, t=2 h)	r=0.2	r=0.4	r=0.6	r=0.8
S3 (P=100, r=0.4)	t=1 h	t=2 h	t=4 h	t=6 h

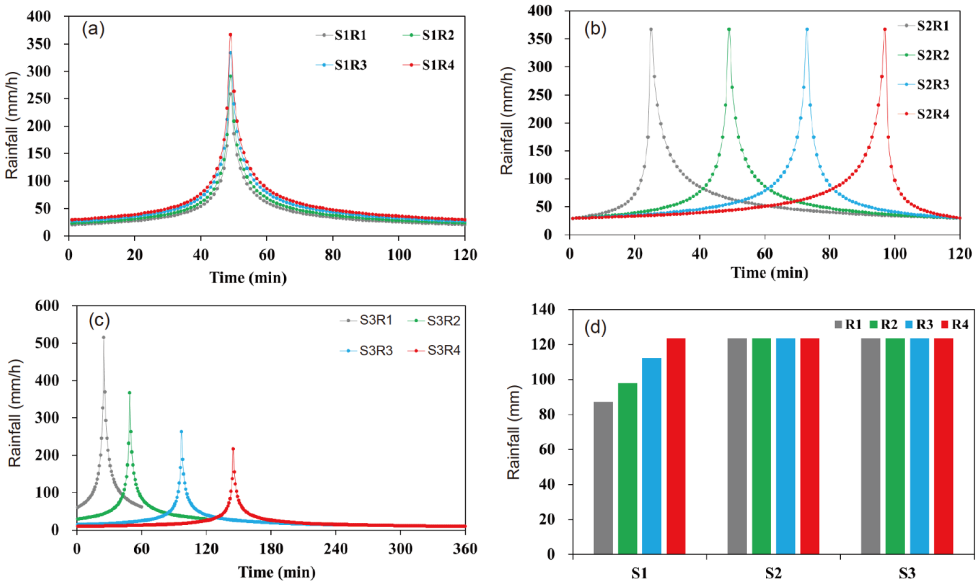

Figure 4 (Color online) 12 design rainstorm events were considered in the scenario analysis which reflects (a) different return periods, (b) different rain patterns, (c) different rainfall durations, and (d) different amounts of total rainfall.

ponents; v_e is the momentum diffusion coefficient; Z is the free-surface elevation. In these equations, h, u, and v are the unknowns to be determined. Full details are provided by Hervouet [44].

TELEMAC-2D also has a rainfall-runoff module. The SCS method was selected for use in simulating the flow generation, and the confluence process of net rain on the surface was simulated using the 2D hydrodynamic method [44]. In the SCS method, the CN value is used to describe the infiltration capability. The main factors of influence on the CN value are the hydrological soil group, land use, hydrologic surface conditions, and antecedent moisture conditions. The basic formulas for the SCS method are as follows:

$$Q = \frac{(P-I_a)^2}{(P-I_a+S)}, \tag{4}$$

$$S = 25.4 \times \left(\frac{1000}{CN} - 10\right), \tag{5}$$

where P is the rainfall depth, mm; Q is the surface runoff, mm; I_a is the initial abstraction, mm; and S is the potential maximal retention, mm.

The BlueKenue software was used to process the basic data. The T3 Mesh tool was used to generate triangular meshes of the study area, with a total of 174310 nodes and 346862 meshes. In consideration of the tradeoff between the computational efficacy and model performance, all of the spatial data were resampled to a 30 m resolution. In addition, they were assigned to triangle unstructured meshes to participate in hydrodynamic simulation calculations. The boundary condition was set to the free outflow boundary by the model. This means the water could have a free flow outside of the study area under gravity. The time step was set to 0.5 s. After several numerical experiments, the Courant-Friedrichs-Lewy (CFL) number was set to 0.75 to ensure the results achieved convergence. In addition, the antecedent moisture condition was set to AMC-II, according to the SCS-CN method. The effect of drainage was considered by converting the design drainage capacity of Xiamen Island into an equivalent rainfall value and deducting it from the design rainstorm to obtain the design rainfall process. The design drainage pipe standard for Xiamen Island is that for a 1-yr storm, which is equal to 0.425 mm/min. In other words, when the rainfall intensity is less than 0.425 mm/min, there is no runoff process in the urban flood model for Xiamen Island. According to some related publications [43,46,47], when considering the climate, hydrologic, and topographic conditions, the Manning coefficients and CN values for the Xiamen Island model are shown in Tables 2 and 3. The detailed process of the model building could refer to ref. [39].

2.3 Damage assessment method

Based on the results of a study of the urban flood disaster vulnerability curve, the maximum inundation depth was selected as the decisive factor in disaster damage assessment [48]. The estimation formula for urban building land flood damage losses in major cities in China [24] is as follows:

$$D = 2.7(h-15)^{0.7998} + 0.95(h-15)^{1.1542} \quad (h > 15), \tag{6}$$

where D is the flood damage losses, Chinese Yuan (CNY); and h is the water depth, cm. Because an urban building is typically 15 cm above the outdoor ground during an actual flood, according to design specifications for outdoor drai-

Table 2 Manning coefficients for different land use types on Xiamen Island

Land use type	Manning coefficient
Woodland	0.08
Road	0.05
Water	0.015
Building	0.2
Other	0.05

Table 3 CN values for different land use types and hydrological soil groups on Xiamen Island

Land use type	Type B	Type C	Type D
Woodland	57	71	80
Road	92	94	98
Water	98	100	100
Building	94	96	98
Other	80	88	92

nage, in the damage calculation, 15 cm was subtracted from the depth of the accumulated water [24]. By applying the damage loss statistics, in combination with the simulation results and the above-mentioned damage assessment formula, the damage loss per unit area, i.e., the damage intensity, was calculated. The total damage of building land was obtained by combining the corresponding cell area statistics.

The lack of observed data in studies related to urban flood simulations is a significant problem. When there is little measured data, it is common practice to analyze the applicability of the constructed model from the rationality of the simulation results. This study also faces the problem of lacking data in constructing the urban flood model of Xiamen Island. Therefore, it is difficult to calibrate and verify the model. However, the applicability of the model has been confirmed from other aspects. The first aspect is the consistency between the simulation results and the actual situations, which is based on the results from the scenario simulations. It could be determined that the locations of the inundation areas are mostly consistent with the location of the actual flooding events that are reported in the historical records. This qualitatively illustrates that the model has rationalities for flood simulations. In addition, based on the simulation results of the different rainfall events, the runoff coefficients are between 0.6 and 0.8. This is also in line with the general situation of the urban areas. Based on the above analysis and the objective purpose of this study, the Xiamen Island urban flood model can meet the basic needs of the scenario analysis in this study. However, its accuracy (i.e. the simulation for actual floods) requires further research.

3 Results

3.1 Flood inundation simulation results

Figure 5(a)–(c) displays the variation of the total flood volume amount (TFVA) in Xiamen Island over time for 12 scenarios. It can be seen from Figure 5(a) that TFVA generally increases with time and then decreases. The TFVA increases at a greater rate in comparison to the period where the TFVA decreases; thus, the peak value of TFVA increases significantly during the design rainstorm return periods. Figure 5(b) demonstrates that although the total amount of rainfall is the same in the scenarios, the difference in the rain

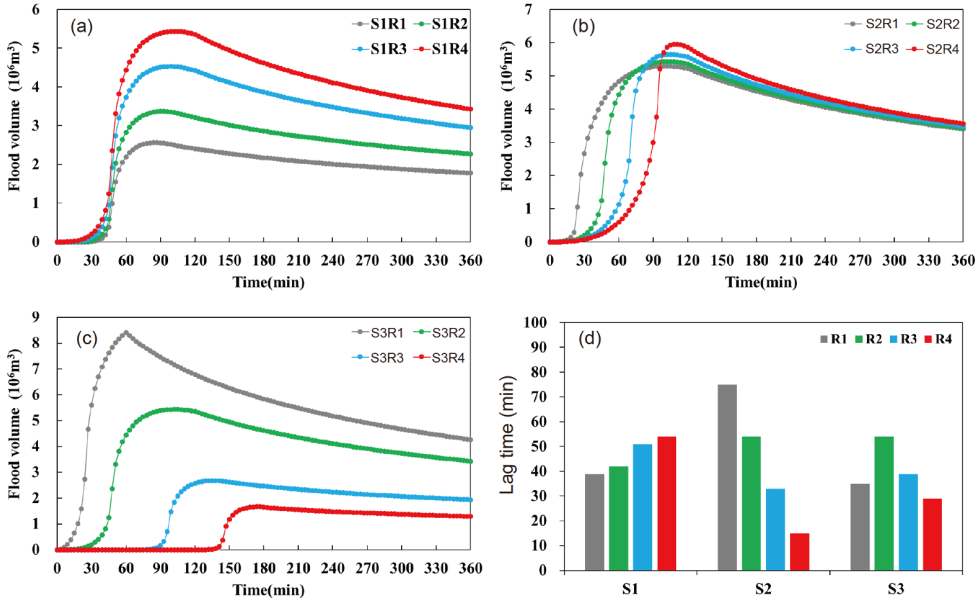

Figure 5 (Color online) Statistical results for the 12 design storm scenarios. The total flood volume amounts for the 12 design storm scenarios (a)–(c) and the lag time (d).

peak coefficient could cause the TFVA change process to be significantly different. The basic rule is that the larger the rain peak coefficient is, the larger the peak value of the corresponding TFVA is. The peak coefficient increased from 0.2 to 0.8, and the peak value of the corresponding TFVA increased from 5.29×10^6 to 5.95×10^6 m^3, with an increase rate of 12.5%. Figure 5(c) demonstrates that the longer the duration of a rainfall is for the same total rainfall amount, the smaller the corresponding TFVA is. For rainfall durations equal to 1, 2, 4, and 6 h, the peak values of the corresponding TFVA are 8.41×10^6, 5.43×10^6, 2.68×10^6, and 1.66×10^6 m^3, respectively, with an average decreasing rate of 41.4%.

The difference between the peak rainfall time and the peak TFVA time was recorded as the lag time in this study, which is an important factor in urban flood prevention. Figure 5(d) shows the lag time for different rainfall scenarios. For the S1 scenario (r=0.4, t=2 h), the lag time increases as the rainfall return period increases. For return periods equal to 1, 2, 4, and 6 h, the peak value of the corresponding lag time is 39, 42, 51, and 54 min, respectively, with an average decreasing rate of 11.7%. In the S2 scenario (P=100, t=2 h), the lag time decreases significantly with an increasing rain peak coefficient. This decreases from 75 to 15 min when the rain peak coefficient increases from 0.2 to 0.8, with an average decreasing rate as high as 80%.

Table 4 summarizes the different levels of the inundation areas associated with the 12 rainfall events. The quantitative results given in this table reflect the impact of different rainfall characteristics on the inundation area. The statistical results for the S1 scenario (r=0.4, t=2 h) indicate that for the 10-yr and 20-yr return periods, the inundation area for the inundation results in a scale of 0.05–0.1. This accounts for the largest proportions, i.e. 16% and 13% of the study area, respectively. For the 50-yr and 100-yr design rainstorm events, the inundation areas at a scale of 0.1–0.2 is the largest, which accounts for 14% and 13% of the study area, respectively. In general, the total area inundation (h>0.05) increases significantly by increasing the design rainstorm return period. The ratio of the inundated area to the study area increases from 22% to 26% as the design rainstorm return period increases from 2 yr to 100 yr. In the S2 scenario (P=100, t=2 h), the inundation area under the 0.1–0.2 level is the largest, and when the rain peaks are equal to 0.2, 0.4, 0.6, and 0.8, the ratios of the inundation area to the study area are 12.8%, 13.2%, 14%, and 15%, respectively. Furthermore, the total inundated area (h>0.05) increases with an increasing rain peak coefficient. In addition, the ratio of the total inundated area to the study area increases from 26% to 29% as the design rainstorm return period increases from 2-yr to 100-yr. The statistical results for the S3 scenario (P=100, r=0.4) indicates that for the 1-h duration rainfall events, the inundation area at the 0.2–0.3 level accounts for the largest proportion, i.e., 20% of the study area. For the 2-h duration events, the inundation area at the 0.1–0.2 level is the largest, which accounts for 13% of the study area. For the 4-h and 6-h events, the inundation areas at the 0.05–0.1 levels account for the largest proportions, 16% and 9% of the study area, respectively. Overall, the total inundated area (h>0.05) decreases significantly as the rainfall duration increases. In addition, the ratio of the total inundated area decreases from 30% for a 1-h duration to 11% for a 6-h, which decreases by a rate of 63%.

In this study, it was assumed that a submergence of 15 cm was the standard for normal waterlogging and that 0.30 m was the standard for severe waterlogging. The statistical results are shown in Figure 6. For the S1 scenario (r=0.4, t=2 h), the areas of normal waterlogging and severe waterlogging increased significantly as the design rainstorm return period increased. This indicates that the rainfall return period (i.e., the rainfall amount and intensity) is an important factor that affects urban inundation. For the S2 scenario (P=100, t=2 h), the areas of normal waterlogging and severe waterlogging do not change essentially with the rain peak coefficient. This indicates that the rain peak coefficient has less influence on high-water-level inundation. For the S3 scenario (P=100, r=0.4), the areas of normal waterlogging and severe waterlogging decreases significantly as the rainfall duration increases for a given rainfall amount. These results indicate that the rainfall duration is an important factor that affects the inundation area for a given rainfall amount.

Figure 7 depicts the spatial distribution of the largest area of inundation for the 12 different design rainstorm scenarios. As illustrated in Figure 7, for the S1 scenario (r=0.4, t=2 h), the inundation area and the maximum water depth increase

Table 4 Statistical results for the inundated area with various depth ranges for the 12 scenarios (%)

Grade	h (m)	S1R1	S1R2	S1R3	S1R4	S2R1	S2R2	S2R3	S2R4	S3R1	S3R2	S3R3	S3R4
I	0.05–0.1	15.9	13.3	6.7	5.4	5.5	5.4	5.3	5.5	4.6	5.4	16.1	9.0
II	0.1–0.2	5.3	9.5	14.2	13.2	12.8	13.2	14.3	15.6	8.6	13.2	5.7	1.8
III	0.2–0.3	0.6	1.4	3.3	5.2	5.1	5.2	5.1	5.7	9.9	5.2	0.7	0.2
IV	0.3–0.4	0.1	0.3	1.1	1.7	1.5	1.7	1.9	1.7	3.8	1.7	0.1	0.0
V	0.4–0.5	0.1	0.1	0.2	0.5	0.5	0.5	0.7	0.8	2.3	0.5	0.1	0.0
VI	>0.5	0.0	0.0	0.1	0.1	0.1	0.1	0.1	0.1	0.5	0.1	0.0	0.0
Total	>0.05	22.0	24.6	25.5	26.1	25.5	26.1	27.3	29.3	29.6	26.1	22.8	11.0

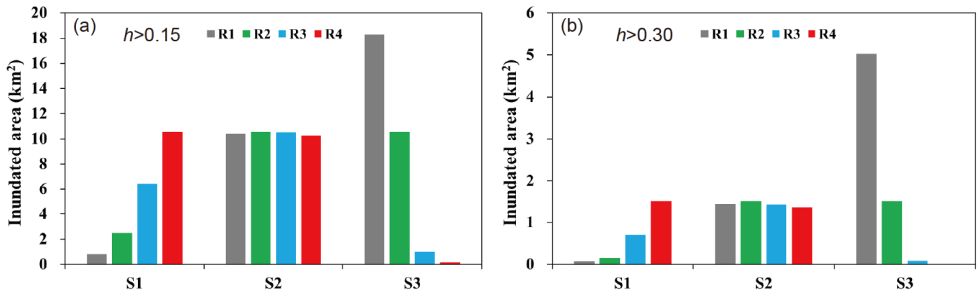

Figure 6 (Color online) Statistical results for the inundation area for the 12 design storm scenarios. (a) Normal waterlogging; (b) severe waterlogging.

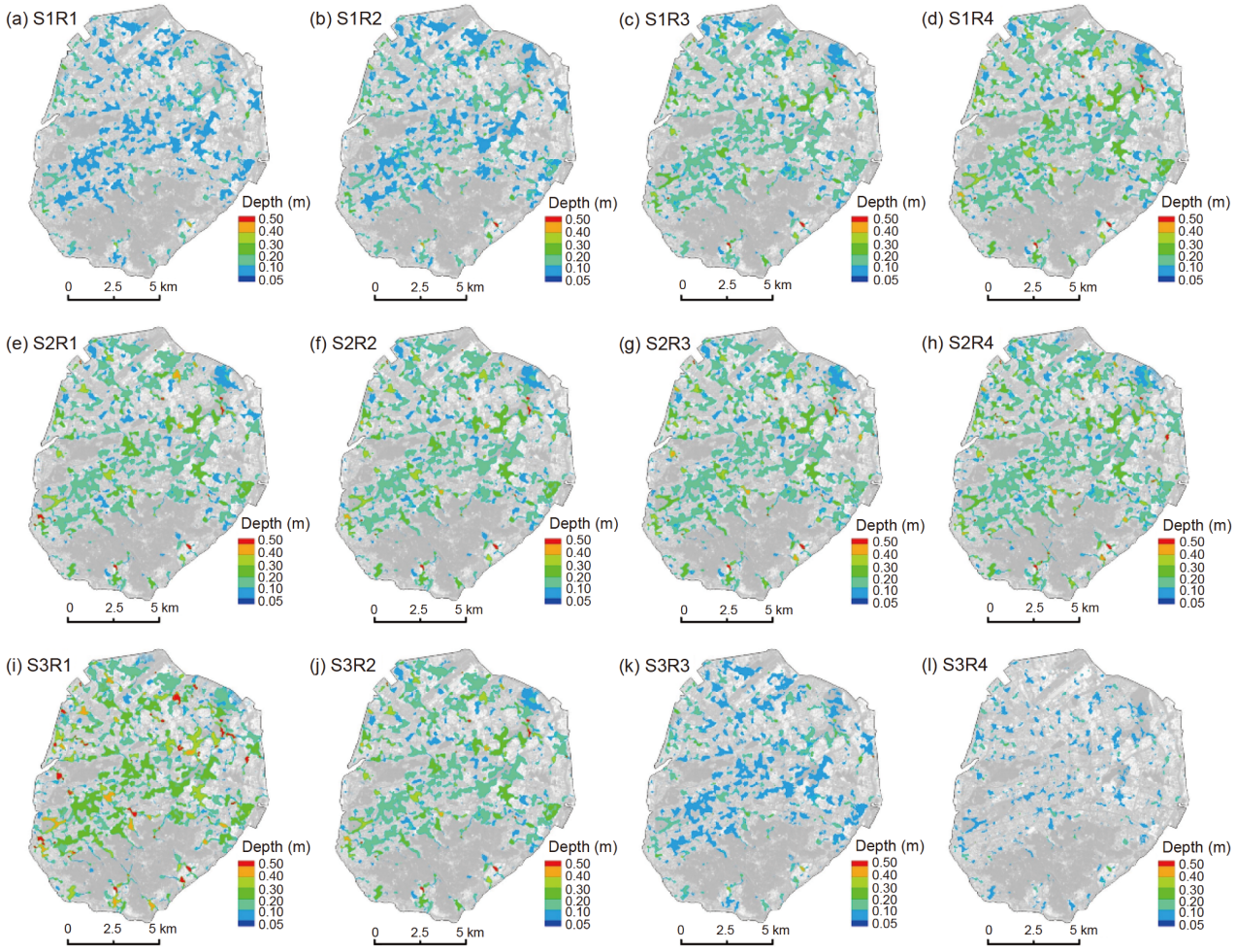

Figure 7 (Color online) Flood inundation maps for the 12 design storm scenarios (a)–(l).

as the rainfall return period increases. For the S2 scenario (P=100, t=2 h), the inundation water distribution does not change with the rain peak coefficient. For the S3 scenario (P=100, r=0.4), both the inundation area and maximum water depth decrease significantly as the rainfall duration increases. Based on the spatial distribution of the inundation area for the 12 rainfall events, the positions of the inundation remain unchanged. These findings provide a possible explanation for why the distribution of the inundation does not change significantly for different rainfall characteristics and TFVAs. This indicates that the inundation area and the maximum water depth vary considerably with the rainfall characteristics.

3.2 Flood inundation damage assessment

In terms of the effects on human socioeconomic systems, researchers are more concerned with damage losses caused

by urban inundation than with TFVA, inundation area, and maximum water depth. Therefore, a damage calculation formula commonly used in China was used to calculate the urban flood disaster damage quantities on building land for different characteristic rainfall events.

Damage intensities for the building land were calculated using eq. (6). The results are presented in Figure 8. For the S1 scenario (r=0.4, t=2 h), the damage intensity increases significantly as the design rainstorm return period increases. For the S2 scenario (P=100, t=2 h), the damage intensity increases slightly as the rain peak coefficient increases. For the S3 scenario (P=100, r=0.4), the damage intensity decreases significantly as the rainfall duration increases. In general, the spatial distributions of damage intensity were similar for the three scenarios; however, the areas were smaller than the spatial distribution of the inundation area. This is because it was assumed that the damage was equal to 0 when the water depth was less than 15 cm and that damage losses occurred only when the water depth was greater than 15 cm.

By multiplying the damage intensity of each grid by the corresponding area and accumulating the damage losses over the building land of study area, the total disaster damage of the building land for the 12 rainfall events were obtained. The results are shown in Figure 9. For the scenario S1 (r=0.4, t=2 h), the total damage loss associated with the urban inundation of buildings on Xiamen Island increases significantly, from 24.30×10^6 CNY to 249.17×10^6 CNY, where the return period increases from 2-yr to 100-yr. For the scenario S2 (P=100, t=2 h), the total damage loss increases slightly as the rain peak coefficient increases. When the rain peak coefficient is 0.2, the total loss is 241.89×10^6 CNY and the damage loss increases to 279.15×10^6 CNY as the rain peak coefficient increases to 0.8. This results in an average increase in the average rain peak coefficient of 0.1, which corresponds to a damage loss increase of 6.21×10^6 CNY. For the scenario S3 (P=100, r=0.4), the total damage decreases significantly as the rainfall duration increases. When the rainfall duration is 1 h, the damage loss is 638.38×10^6 CNY. When the rainfall duration increases to 6 h, the damage loss is reduced to 5.58×10^6 CNY, with a reduction rate of 99%.

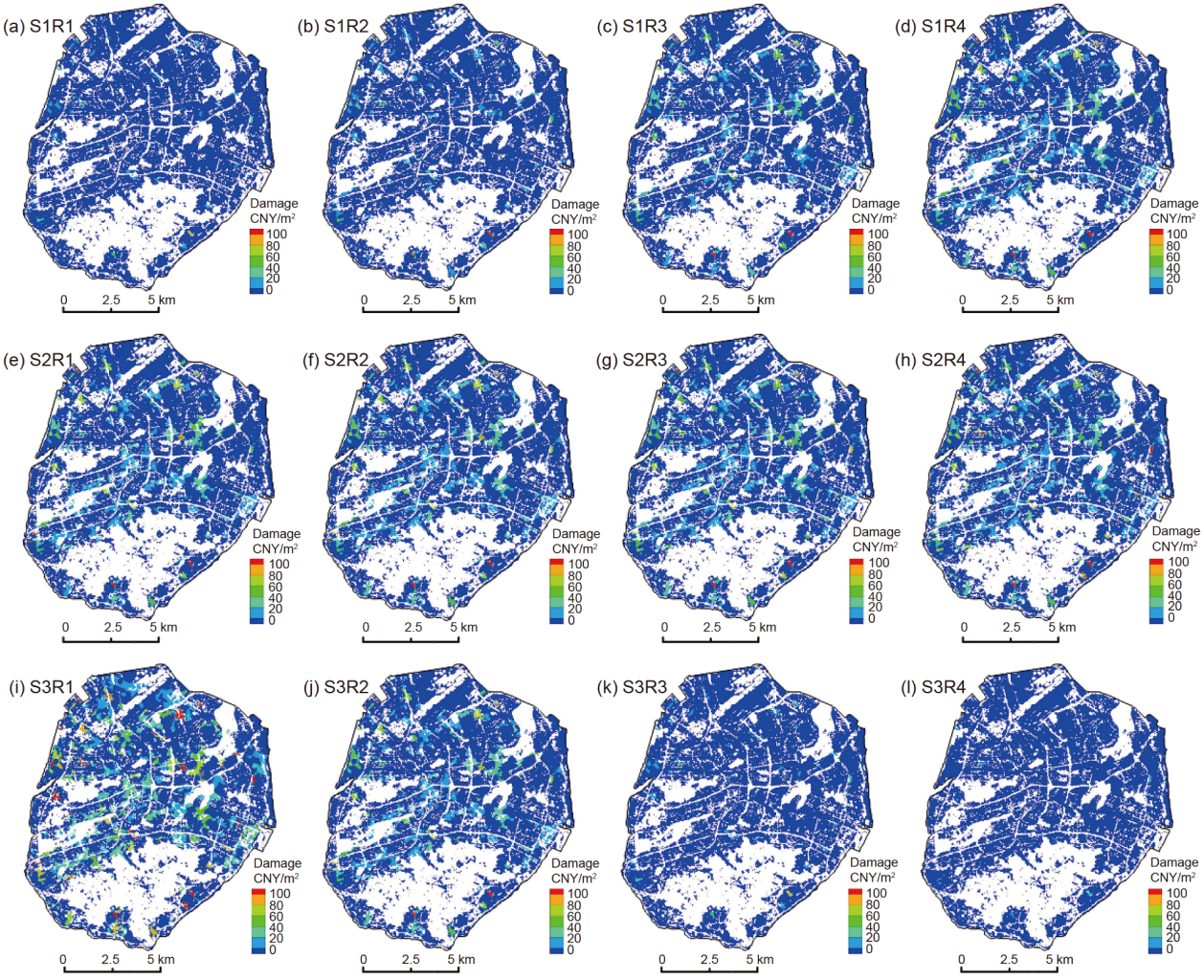

Figure 8 (Color online) Damage loss maps for the building land under 12 design storm scenarios (a)–(l).

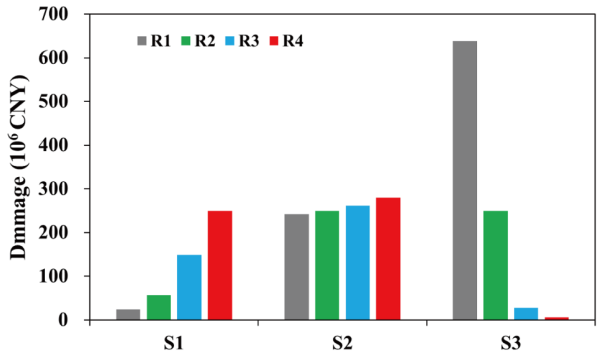

Figure 9 (Color online) Statistical results for building land damage losses under 12 design storm scenarios.

4 Discussion

4.1 Effects of rainfall characteristics and implications for urban flood management

Based on numerical simulations and the analysis of scenarios, the impact of design rainstorm characteristics on urban flooding and disaster damage were examined quantitatively in this study. This research focused on three key characteristics of design rainstorms, namely, the rainfall return period, rain peak coefficient, and the rainfall duration. Different return periods correspond to different rainfall intensities and rainfall amounts. Meanwhile, different rainfall durations only represent different rainfall densities and different rain peak coefficients only represent different rainfall patterns for a given rainfall amount.

The quantitative analysis results indicate that the rainfall amount and rainfall intensity are the decisive factors that affect the urban flooding inundation and disaster damage amounts. It is worth noting that the rainfall pattern also significantly affects the flooding and inundation results. This implies that although the total amount of rainfall and the rainfall duration are the same, different rainfall processes will produce different results. This study reveals that a higher rainfall rain peak coefficient results in more severe urban inundation and greater damage losses [49]. A possible explanation for this might be that when the rain peak coefficient is small, the early rainfall intensity is severe, while the soil is not saturated. Therefore, a lot of rainfall can be infiltrated and the inundation is not very severe. When the rain peak coefficient is large, the end of the rainfall intensity is severe even though the soil is almost completely saturated. As a result, heavy rainfall and little infiltration happen at the same time, in which the inundation and damage are severe.

In addition, Figure 5(d) reflects that the rainfall characteristics have a large influence on the lag time. These relationships may partly be explained by the fact based on the following scenarios. For the scenario S1 when the rain peak coefficient is larger, the TFVA is more. In addition, the time of rainfall confluence is longer, which results in a larger lag time. For the scenario S2 in the latter of the rainfall, the heavy rainfall and severe inundation happened simultaneously; therefore, the lag time is small. For the scenario S3 the lag time of 2 h is larger than others. As a result, these phenomena are likely to be related to the terrain and the flow confluence takes some time to accumulate water under gravity. Further research with more focus on the lag time is suggested. These results suggest that researchers should pay more attention to changing rainfall patterns [50] to prevent damage due to urban flooding. Furthermore, for urban stormwater infrastructure planning and design, it is necessary to consider the local rainstorm characteristics to balance the safety and economy, which is essential for selecting a rainstorm design. In China, the design rainstorm peak coefficient for an urban design rainstorm is usually in the range of 0.3–0.5. However, this research indicates that the larger the coefficient is for a rainstorm, the more damage losses there are. Therefore, in consideration of infrastructure safety, it is suggested that it is better to set a larger rain peak coefficient when it comes to urban drainage infrastructure design.

In the current context of climate change and rapid urbanization, many studies have shown that there is an increasing trend of rainfall in urban areas, which may lead to severe urban flooding [51,52]. The results of this study suggest that it is better to analyze the impact of rainfall changes for urban stormwater. Researchers should pay attention to changes in rainfall, rainfall patterns, and rainfall intensity as well as trends related to extreme rainfall within short time durations [53]. Extreme rainfall is the most dangerous hazard factor for urban flooding; hence it is better to respond to rainfall events that may result in urban flooding. In addition, the scale of rainfall forecasting and evolution studies should be reduced from years and days to hours. In summary, the results of this study indicate that the formulation of urban flood prevention and management strategies should be based on the results of well-designed studies for urban rainfall characteristics.

From the perspective of urban stormwater risk control strategies, the distributions of urban inundations have some similarities. It is necessary to prevent flood disasters caused by greater inundation depths, and this can be forecasted to some extent. However, the results indicate that different measures should be conducted to prevent rainstorms with different characteristics. For example, rainstorms with a large rain peak coefficient and a long duration, the lag time between the peak rainfall and peak runoff would be short. In other words, the response time is very short and quick relief operations are vital for flood prevention. For rainstorms with a larger return period or a shorter duration, the inundation area and TFVA will be large according to the numerical results; therefore, pumps or other drainage facilities are important for flood management. When it is expected that severe inundation may occur, personnel and property evacuation should be organized to minimize property losses.

This requires that people make corresponding plans based on possible flooding forecasts. At the same time, it is necessary to improve the risk management of urban floods. Cities are encouraged to formulate urban flood risk maps and should conduct urban flood risk warnings based on numerical simulations [54,55]. In addition, for the foreseeable affected areas and targets of urban flood disaster risks, an insurance system should also be introduced to force the purchase of urban rainwater disaster insurance. This will make use of social capital disaster relief, enhance the city's resilience when facing flood disasters, and reduce the burden of urban flood disasters for the government and its citizens.

4.2 Limitations and future studies

Given the lack of detailed data available, some model simplifications had to be made in this study. As a result, these simplifications may have created some uncertainties in the simulation results [18]. First, simulation of the drainage pipe network was not considered in this study. Therefore, a simplified method was used to estimate an equivalent deduction for flooding due to drainage. This method is a common generalization method that was used in the absence of pipe network data; however, it has some limitations. On the one hand, it is inconsistent with the actual situation because the spatial and temporal changes in the drainage capacity are neglected. This is because the complex flow regime of the drainage network is not considered in detail. On the other hand, the drainage flow process cannot be considered after the rain has ended. However, the limitations of this method do not affect the credibility and universality of the conclusions for this study. One reason for this is that the rainfall intensities of the 12 rainfall events considered in this study were relatively high. The drainage pipe network would be full during high-intensity rainfalls. This is consistent with the design value considered in the simplified method, which makes the generalization reasonable [56,57]. In addition, the focus in this study was primarily on the state when the degree of inundation reaches a maximum and less on the process of flooding accumulation. In particular, this study explored the process of flood subsidence. It is worth noting that only the flood damage for building land in an urban flood was analyzed in this study. This was the main loss among all of the kinds of land use types. Moreover, the conclusions that were drawn are based on comparisons of the 12 design rainstorm scenarios; thus, ensuring the reliability of the conclusions. The most important point is that conclusions were drawn from this study based on the comparisons of the scenario simulations. In other words, the generalization that was previously described is offset to some extent, which reinforces the credibility of the research results that were achieved in this study.

In terms of the parameters, input data, and structure of the constructed model, the simulation results also have some uncertainties [18,34]. First, in the simulation of basic data and boundary conditions, given the lack of detailed measured data, the actual situations of pumping stations, reservoirs, rivers, and tides were not considered. In addition, actual flooding data was not used to verify the simulation results. The parameters, input data, and structure of the model also introduced uncertainties to some extent. Quantifying, exploring, and resolving these uncertainties need to be explored in future research efforts.

The results of this study show that performing numerical simulations is a useful way to reduce the cost of experiments and to obtain results for a large number of urban flooding scenarios that can be used to improve urban stormwater management. By conducting numerical simulations, this is an important tool in assessing the urban stormwater conditions; research on monitoring datasets is generally lacking and it is difficult to obtain this data [34].

Our future research will be focused on collecting more measured data, improving the modeling methods and structure, and building more appropriate models that better reflect actual conditions in urban areas. These efforts will support more refined simulations to combat urban flooding [18].

5 Conclusions

In this study, a numerical model was used to explore the effects of design rainstorm characteristics on inundation indexes and disaster damage levels. Based on the results of the numerical simulations and scenario analyses, the following conclusions were drawn.

(1) The rainfall amount, rainfall pattern, and rainfall intensity are important factors in urban inundation. In general, the higher the rainfall peak coefficient is and the shorter the rainfall duration is, the more severe urban inundation and damage occurs for a given amount of rainfall. Furthermore, the greater the rainfall amount and the rainfall intensity are, the greater the inundation area is in proportion to the high-level inundation depth. The study results show that the rainfall intensity and rainfall pattern are important factors that affect urban inundation.

(2) The lag time between the rainfall peak and flood volume peak increases significantly as the rainfall return period increases, and it decreases as the rain peak coefficient increases. However, there is no clear relationship between the lag time and rainfall duration. The influence of the rain peak coefficient on the lag time is apparent. When the rain peak coefficient increases from 0.2 to 0.8, the lag time decreases from 75 to 15 min. For that, the lag time is closely related to the disaster response time. This finding is meaningful for the rational formulation of urban flooding management strategies.

(3) For the purpose of damage loss assessment, it is relevant that damage losses increased significantly as the return period of the design rainstorm increased. For the same rainfall amount, the disaster damages increased slowly as the rain peak coefficient increased. However, it decreased significantly as the rainfall duration increased. When the rain duration increased from 1 to 6 h, the damage losses were reduced by 99%. This indicates that the rainfall intensity is an important factor that can have an influence on the damage, whereas the impact of the rainfall pattern is slightly weaker.

This work was supported by the National Natural Science Foundation of China (Grant Nos. 51739011 & 51879274), the National Key Research and Development Program of China (Grant Nos. 2018YFC1508203 & 2016YFC0401401).

1 Zhang W, Villarini G, Vecchi G A, et al. Urbanization exacerbated the rainfall and flooding caused by hurricane Harvey in Houston. Nature, 2018, 563: 384–388
2 Hallegatte S, Green C, Nicholls R J, et al. Future flood losses in major coastal cities. Nat Clim Change, 2013, 3: 802–806
3 Guan X, Wei H, Lu S, et al. Assessment on the urbanization strategy in China: Achievements, challenges and reflections. Habitat Int, 2018, 71: 97–109
4 Zhou Q, Leng G, Su J, et al. Comparison of urbanization and climate change impacts on urban flood volumes: Importance of urban planning and drainage adaptation. Sci Total Environ, 2019, 658: 24–33
5 Jiang Y, Zevenbergen C, Ma Y. Urban pluvial flooding and stormwater management: A contemporary review of China's challenges and "sponge cities" strategy. Environ Sci Policy, 2018, 80: 132–143
6 Xu H, Ma C, Lian J, et al. Urban flooding risk assessment based on an integrated *k*-means cluster algorithm and improved entropy weight method in the region of Haikou, China. J Hydrol, 2018, 564: 975–986
7 Chen S Y, Xue Z C, Li M, et al. Variable sets method for urban flood vulnerability assessment. Sci China Tech Sci, 2013, 56: 3129–3136
8 Xia J, Zhang Y Y, Xiong L H, et al. Opportunities and challenges of the Sponge City construction related to urban water issues in China. Sci China Earth Sci, 2017, 60: 652–658
9 Jameson S, Baud I. Varieties of knowledge for assembling an urban flood management governance configuration in Chennai, India. Habitat Int, 2016, 54: 112–123
10 Quan J L. Enhanced geographic information system-based mapping of local climate zones in Beijing, China. Sci China Tech Sci, 2019, 62: 2243–2260
11 Huang H, Chen X, Zhu Z, et al. The changing pattern of urban flooding in Guangzhou, China. Sci Total Environ, 2018, 622-623: 394–401
12 Wang H, Mei C, Liu J H, et al. A new strategy for integrated urban water management in China: Sponge city. Sci China Tech Sci, 2018, 61: 317–329
13 Gao L, Huang J, Chen X, et al. Contributions of natural climate changes and human activities to the trend of extreme precipitation. Atmos Res, 2018, 205: 60–69
14 Pathirana A, Denekew H B, Veerbeek W, et al. Impact of urban growth-driven landuse change on microclimate and extreme precipitation—A sensitivity study. Atmos Res, 2014, 138: 59–72
15 Hailegeorgis T T, Thorolfsson S T, Alfredsen K. Regional frequency analysis of extreme precipitation with consideration of uncertainties to update IDF curves for the city of Trondheim. J Hydrol, 2013, 498: 305–318
16 Hodgkins G A, Dudley R W, Archfield S A, et al. Effects of climate, regulation, and urbanization on historical flood trends in the United States. J Hydrol, 2019, 573: 697–709
17 Suttles K M, Singh N K, Vose J M, et al. Assessment of hydrologic vulnerability to urbanization and climate change in a rapidly changing watershed in the Southeast U.S.. Sci Total Environ, 2018, 645: 806–816
18 Luo P, Mu D, Xue H, et al. Flood inundation assessment for the Hanoi Central Area, Vietnam under historical and extreme rainfall conditions. Sci Rep, 2018, 8: 12623
19 Chen X B, Wang Y C, Ni J R. Structural characteristics of river networks and their relations to basin factors in the Yangtze and Yellow River basins. Sci China Tech Sci, 2019, 62: 1885–1895
20 Molinari D, Ballio F, Handmer J, et al. On the modeling of significance for flood damage assessment. Int J Disaster Risk Reduction, 2014, 10: 381–391
21 Scawthorn C, Blais N, Seligson H, et al. HAZUS-MH flood loss estimation methodology. I: Overview and flood hazard characterization. Nat Hazards Rev, 2006, 7: 60–71
22 Jamali B, Löwe R, Bach P M, et al. A rapid urban flood inundation and damage assessment model. J Hydrol, 2018, 564: 1085–1098
23 Hammond M J, Chen A S, Djordjević S, et al. Urban flood impact assessment: A state-of-the-art review. Urban Water J, 2015, 12: 14–29
24 Yin Z E, Xu S Y. Study on Risk Assessment of Urban Natural Hazards (in Chinese). Beijing: Science Press, 2012
25 Qin H, Li Z, Fu G. The effects of low impact development on urban flooding under different rainfall characteristics. J Environ Manage, 2013, 129: 577–585
26 Goodarzi L, Banihabib M E, Roozbahani A. A decision-making model for flood warning system based on ensemble forecasts. J Hydrol, 2019, 573: 207–219
27 Glenis V, Kutija V, Kilsby C G. A fully hydrodynamic urban flood modelling system representing buildings, green space and interventions. Environ Model Software, 2018, 109: 272–292
28 Zhou Y, Shen D, Huang N, et al. Urban flood risk assessment using storm characteristic parameters sensitive to catchment-specific drainage system. Sci Total Environ, 2019, 659: 1362–1369
29 Czajkowski J, Engel V, Martinez C, et al. Economic impacts of urban flooding in South Florida: Potential consequences of managing groundwater to prevent salt water intrusion. Sci Total Environ, 2018, 621: 465–478
30 Mei C, Liu J, Wang H, et al. Integrated assessments of green infrastructure for flood mitigation to support robust decision-making for sponge city construction in an urbanized watershed. Sci Total Environ, 2018, 639: 1394–1407
31 Seenath A, Wilson M, Miller K. Hydrodynamic versus GIS modelling for coastal flood vulnerability assessment: Which is better for guiding coastal management? Ocean Coast Manage, 2016, 120: 99–109
32 Neal J, Dunne T, Sampson C, et al. Optimisation of the two-dimensional hydraulic model LISFOOD-FP for CPU architecture. Environ Model Software, 2018, 107: 148–157
33 Li W, Lin K, Zhao T, et al. Risk assessment and sensitivity analysis of flash floods in ungauged basins using coupled hydrologic and hydrodynamic models. J Hydrol, 2019, 572: 108–120
34 Teng J, Jakeman A J, Vaze J, et al. Flood inundation modelling: A review of methods, recent advances and uncertainty analysis. Environ Model Software, 2017, 90: 201–216
35 Brière C, Abadie S, Bretel P, et al. Assessment of TELEMAC system performances, a hydrodynamic case study of Anglet, France. Coast Eng, 2007, 54: 345–356
36 Moulinec C, Denis C, Pham C T, et al. TELEMAC: An efficient hydrodynamics suite for massively parallel architectures. Comput Fluids, 2011, 51: 30–34
37 Vachaud G, Quertamp F, Phan T S H, et al. Flood-related risks in Ho Chi Minh City and ways of mitigation. J Hydrol, 2018, 573: 1021–1027
38 Chen S, Zha X. Effects of the ENSO on rainfall erosivity in the Fujian Province of southeast China. Sci Total Environ, 2018, 621: 1378–1388
39 Liu J H, Li Z J, Mei C, et al. Urban flood analysis for different design storm hyetographs in Xiamen Island based on TELEMAC-2D. Chin

Sci Bull, 2019, 64: 2055–2066
40 Shang H, Lin B, Xu L. Visualization of precipitation frequency atlas & rainstorm high-risk regionalization atlas (in Chinese). China Water Wastew, 2019, 35: 131–138
41 Yin J, Yu D, Yin Z, et al. Evaluating the impact and risk of pluvial flash flood on intra-urban road network: A case study in the city center of Shanghai, China. J Hydrol, 2016, 537: 138–145
42 Balbastre-Soldevila R, García-Bartual R, Andrés-Doménech I. A comparison of design storms for urban drainage system applications. Water, 2019, 11: 757–771
43 Keifer C J, Chu H H. Synthetic storm pattern for drainage design. J Hydraul Div, 1957, 83: 1–25
44 Hervouet J M. Hydrodynamics of Free Surface Flows: Modelling with the Finite Element Method. Chichester: John Wiley & Sons, 2007. 83–133
45 Hervouet J M. TELEMAC modelling system: An overview. Hydrol Process, 2000, 14: 2209–2210
46 Lin M. Study on rainstorm waterlogging disaster risk base on the construction of sponge city: A case study of Xiamen (in Chinese). Dissertation for Master's Degree. Xi'an: Xi'an University of Science and Technology, 2014
47 Wang D, Qin L, Chang B, et al. Application of SCS-CN model in runoff estimation. In: 2015 International Symposium on Material, Energy and Environment Engineering. Paris: Atlantis Press, 2015
48 Su B, Huang H, Zhang N. Dynamic urban waterlogging risk assessment method based on scenario simulations (in Chinese). J Tsinghua Univ (Sci Tech), 2015, 55: 684–690
49 Chen W, Huang G, Zhang H, et al. Urban inundation response to rainstorm patterns with a coupled hydrodynamic model: A case study in Haidian Island, China. J Hydrol, 2018, 564: 1022–1035
50 Li Z, Li X, Wang Y, et al. Impact of climate change on precipitation patterns in Houston, Texas, USA. Anthropocene, 2019, 25: 100193
51 Sofia G, Roder G, Dalla Fontana G, et al. Flood dynamics in urbanised landscapes: 100 years of climate and humans' interaction. Sci Rep, 2017, 7: 40527
52 Villarini G, Smith J A, Lynn Baeck M, et al. Radar analyses of extreme rainfall and flooding in urban drainage basins. J Hydrol, 2010, 381: 266–286
53 Faccini F, Luino F, Paliaga G, et al. Role of rainfall intensity and urban sprawl in the 2014 flash flood in Genoa City, Bisagno catchment (Liguria, Italy). Appl Geogr, 2018, 98: 224–241
54 Darabi H, Choubin B, Rahmati O, et al. Urban flood risk mapping using the GARP and QUEST models: A comparative study of machine learning techniques. J Hydrol, 2019, 569: 142–154
55 Liu Z L, Zhou Y W, Liu S S, et al. Approach of building content damage assessment and risk quantification by urban local flooding based on GIS (in Chinese). J Beijing Univ Tech, 2015, 41: 275–280
56 Abily M, Bertrand N, Delestre O, et al. Spatial Global Sensitivity Analysis of High Resolution classified topographic data use in 2D urban flood modelling. Environ Model Software, 2016, 77: 183–195
57 Mignot E, Paquier A, Haider S. Modeling floods in a dense urban area using 2D shallow water equations. J Hydrol, 2006, 327: 186–199